



CHALMERS
UNIVERSITY OF TECHNOLOGY

Measurements of industrial emissions of alkenes in Texas using the solar occultation flux method

Downloaded from: <https://research.chalmers.se>, 2024-07-27 13:49 UTC

Citation for the original published paper (version of record):

Mellqvist, J., Samuelsson, J., Johansson, J. et al (2010). Measurements of industrial emissions of alkenes in Texas using the solar occultation flux method. *Journal of Geophysical Research: Atmospheres*, 115(D7). <http://dx.doi.org/10.1029/2008jd011682>

N.B. When citing this work, cite the original published paper.



Measurements of industrial emissions of alkenes in Texas using the solar occultation flux method

Johan Mellqvist,¹ Jerker Samuelsson,¹ John Johansson,¹ Claudia Rivera,¹ Barry Lefer,² Sergio Alvarez,³ and John Jolly⁴

Received 29 December 2008; revised 7 September 2009; accepted 14 September 2009; published 13 March 2010.

[1] Solar occultation flux (SOF) measurements of alkenes have been conducted to identify and quantify the largest emission sources in the vicinity of Houston and in SE Texas during September 2006 as part of the TexAQS 2006 campaign. The measurements have been compared to emission inventories and have been conducted in parallel with airborne plume studies. The SOF measurements show that the hourly gas emissions from the large petrochemical and refining complexes in the Houston Ship Channel area and Mount Belvieu during September 2006 corresponded to 1250 ± 180 kg/h of ethene and 2140 ± 520 kg/h of propene, with an estimated uncertainty of about 35%. This can be compared to the 2006 emission inventory value for ethene and propene of 145 ± 4 and 181 ± 42 kg/h, respectively. On average, for all measurements during the campaign, the discrepancy factor is $10.2(+8,-5)$ for ethene and $11.7(+7,-4)$ for propene. The largest emission source was Mount Belvieu, NE of the Houston Ship Channel, with ethene and propene emissions corresponding to 440 ± 130 kg/h and 490 ± 190 kg/h, respectively. Large variability of propene was observed from several petrochemical industries, for which the largest reported emission sources are flares. The SOF alkene emissions agree within 50% with emissions derived from airborne measurements at three different sites. The airborne measurements also provide support to the SOF error budget.

Citation: Mellqvist, J., J. Samuelsson, J. Johansson, C. Rivera, B. Lefer, S. Alvarez, and J. Jolly (2010), Measurements of industrial emissions of alkenes in Texas using the solar occultation flux method, *J. Geophys. Res.*, 115, D00F17, doi:10.1029/2008JD011682.

1. Introduction

[2] This study investigates fugitive emissions of ethene and propene, two highly reactive volatile organic compounds (HRVOCs), from industrial sources in the vicinity of Houston. The objective of the study was to locate these sources and quantify their VOC emissions. The work is part of the TexAQS 2006 intensive summer campaign, included in the Second Texas Air Quality Study (TexAQS II), with the aim of better understanding the formation of tropospheric ozone in southeastern Texas. Ozone is formed by photochemical reactions between VOCs and nitrogen oxides. In a previous air quality study in 2000 it was noted that the industries in Texas seem to emit considerably more highly reactive VOCs than reported and that the emissions are important contributors to ozone formation in Texas [Ryerson *et al.*, 2003; Wert *et al.*, 2003]. This was found by conducting airborne measurements downwind of several isolated facilities to determine the ratios of HRVOCs to NO_x . The results

showed discrepancies between reported and measured values of a factor 20 to 70. Assuming the NO_x emissions are better known, which seemed to be the case, the discrepancy is primarily due to higher than reported VOC emissions. This approach is indirect as it relies on the assumption that the NO_x emissions are known and that the HRVOCs and NO_x is mixed uniformly in the plume. The latter is not always the case since the species are released from different parts of the industries, NO_x mostly through stacks and VOCs through fugitive emissions from process equipment. An uncertainty is whether the relatively few measurement days during which the measurements were conducted are representative of the industries' baseline emissions.

[3] To overcome some of the uncertainties with the previous emission studies, a direct method to quantify fugitive emissions has been applied in the TexAQS 2006 study, i.e., the solar occultation flux (SOF) method. It utilizes the Sun as the light source and vertically integrated concentrations of gas species that absorb in the infrared portion of the solar spectrum are measured from a vehicle that travels on roads upwind and downwind of the target sources (0.5 to 3 km distance). The gas fluxes are obtained by multiplying the mass across the plume with the wind speed. This approach of obtaining the gas flux is similar to other methods used to measure volcanic fluxes of SO_2 , for instance scanning passive ultraviolet measurements [Galle *et al.*, 2003], the laser based technique DIAL [Weibring *et al.*, 1998] and DOAS and COSPEC, two mobile techniques

¹Radio and Space Science, Chalmers University of Technology, Göteborg, Sweden.

²Department of Geosciences, University of Houston, Houston, Texas, USA.

³Institute for Air Science, Baylor University, Waco, Texas, USA.

⁴Texas Commission on Air Quality, Austin, Texas, USA.

using zenith scattered UV light [Weibring *et al.*, 1998]. The DIAL technique is also applied for measurement of VOC emissions from industries [Walmsley and O'Connor, 1998].

[4] In this paper the 2006 SOF data has been compared to emission inventories developed by the TCEQ (Texas Commission on Environmental Quality) for 2006. The SOF data has also been compared to emission values estimated from the NOAA WP-3D aircraft and the Baylor Piper Aztec airplane, measuring in parallel with the SOF. Furthermore, the airborne data has been used to analyze the vertical mixing of the gas plumes. This is of relevance for the estimation of the measurement uncertainty for the SOF measurements. More information can be found in two recent reports [Mellqvist *et al.*, 2007; 2008]. Simultaneous measurements of NO₂ and SO₂ were also conducted with a UV/visible system and these will be published elsewhere [Rivera *et al.*, 2010] as well as SOF alkane emission measurement (J. Samuelsson, manuscript in preparation, 2010).

2. Methods

2.1. Measurement Method

[5] The SOF method is relatively new and was developed from research projects involving studies of industrial emissions [Mellqvist, 1999] using long path FTIR (Fourier Transform Infrared) and solar high-resolution FTIR measurements of atmospheric species [Mellqvist, 1999; Mellqvist *et al.*, 2002; Galle *et al.*, 1999] within the NDACC network (Network for Detection of Atmospheric Composition Change, <http://www.ndsc.ncep.noaa.gov>). The method is based on the recording of solar broadband infrared (IR) absorption spectra (1.8–14 μm). The spectral retrieval is similar to that of conventional long path FTIR spectroscopy [Hanst *et al.*, 1982] but due to the long atmospheric path length of the solar light the spectra are characterized by strong absorptions caused by the background atmospheric species such as H₂O, CO₂ and CH₄ and this has to be taken into account in the spectral evaluation. In the infrared region of the solar spectrum a large number of species, such as aldehydes, alkanes, ammonia, CO, ethene, ethane oxide, HF, HCl, SO₂, propene, terpenes, and vinyl chloride, can be measured. The method has been used quite extensively in Sweden [Kihlman *et al.*, 2005; Kihlman, 2005] for VOC measurements of refineries but also for volcanic measurements of SO₂, HCl and HF [Mellqvist *et al.*, 2005] and CO column measurements in megacities [Mellqvist *et al.*, 2004; Foy *et al.*, 2007].

[6] The SOF instrument is built into a van and consists of a custom built solar tracker, transfer optics and a Bruker OPAG FTIR spectrometer with a spectral resolution of 0.5 cm^{-1} , equipped with both an MCT (MercuryCadmiumTelluride) detector, primarily for the 9–14 μm wavelength region, and an InSb (IndiumAntimonide) detector for the 2.5–5.5 μm region. The Sun tracker is a mirror device that tracks the Sun and reflects the light into the spectrometer. Optical interference filters are used to optimize the signal-to-noise ratio (S/N) of the measurements.

[7] The spectral retrieval is conducted by custom software (QESOF) [Kihlman, 2005]. Here, calibration spectra are fitted to the measured spectra using nonlinear multivariate analysis. Calibration data from the HITRAN database

[Rothman *et al.*, 2005] are used to simulate absorption spectra for ethene and other interfering atmospheric background species at the actual pressure, temperature and instrumental resolution of the measurements. The same approach is applied for several retrieval codes for high-resolution solar spectroscopy [Rinsland *et al.*, 1991; Griffith, 1996]. For propene, high-resolution spectra are obtained from the PNL (Pacific Northwest Laboratory) database [Sharpe *et al.*, 2004] and these are degraded to the spectral resolution of the instrument by convolution with the instrument line shape. The uncertainty in the absorption strength of the calibration spectra is about 3% for both species.

[8] The retrieval of ethene is conducted in the wavelength region between 945 and 979 cm^{-1} (10.21–10.58 μm) taking into account the interfering species water and CO₂. Propene is retrieved between 900 and 920 cm^{-1} (10.87–11.11 μm) taking into account interfering absorptions of ethene, ammonia, 1-butene, 1,3-butadiene, CO₂ and H₂O. In the spectral region around 10 μm , warm objects radiate heat which creates a thermal background in the absorption spectrum. To correct for this a thermal background spectrum is recorded at regular intervals by measuring with the solar tracker pointed to the cold sky i.e., away from the Sun. This background spectrum is then subtracted from each recorded solar spectrum. In the spectral retrieval algorithm, a reference spectrum is chosen from a region of the measurement transect where it can be assumed that the target gas concentration is near zero and which corresponds to the lowest column value measured. Instead of calculating the transmittance by dividing all spectra with the reference, which is the common approach in long path FTIR, the logarithm of the reference spectrum is fitted to the measured spectrum together with cross sections of the gas species to be retrieved which are adapted to the instrumental parameters, as shown in equation (1) below, which simply is a rewriting of the Beer Lambert law. This approach makes it possible to account for wavelength shifts in the spectra and also to include several reference spectra in the fit, which results in efficient removal of the influence of the upper atmosphere.

$$\ln[I(\nu)] = \sum_j F_j \cdot \ln[I_{0,j}(\nu)] - \sum_i \sigma_i(\nu) \cdot \int \text{conc}_i(z) \cdot dz. \quad (1)$$

Here, I corresponds to the measured light intensity as a function of frequency ν , $I_{0,j}$ corresponds to reference spectra with fitting factors F_j , σ_i corresponds to cross sections for the fitted species and the last part of equation (1) is the vertically integrated concentration, i.e., column, to be determined.

[9] The results of the spectral fitting algorithm for alkanes have been compared and verified with the results retrieved from the nonlinear NLM4 software developed by Griffith [1996]. The agreement between NLM4 and QESOF is good; it is within a few percent. Verification of the QESOF software has also been conducted for the volcanic species HCl and SO₂ by comparison with a code developed by Burton *et al.* [2001] which shows good agreement, also with differences of within a few percent [Mellqvist *et al.*, 2005]. In Figure 1 solar spectra are shown corresponding to measurements downwind and upwind of an industrial

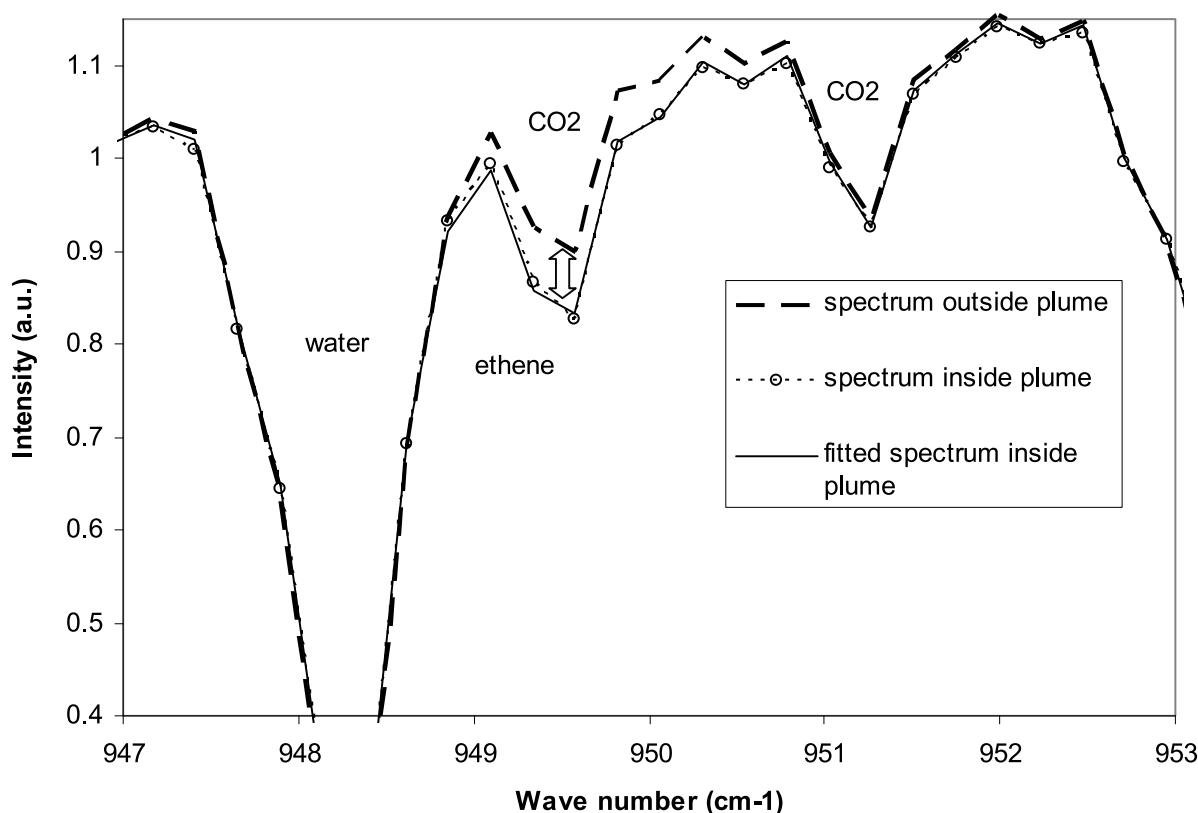


Figure 1. Solar spectra measured outside and inside the emission plume of an industrial plant in arbitrary intensity units. In addition, spectral fits of ethene (upper) obtained using the QESOF spectral retrieval algorithm are shown.

facility in the Houston Ship Channel (HSC). The measurement time of these spectra corresponds to 5 s, which is typical for all measurements presented here. In addition, a spectral fit of ethene, H_2O and CO_2 to the downwind spectrum is shown, using the upwind spectrum as reference. For this case, a clear absorption signal for ethene is shown corresponding to 35 mg/m^2 . The retrieval for ethene has a variability (1σ) of about 0.5 mg/m^2 caused by interference effects and noise due to instrument vibrations and disturbances while driving. For propene the variability is higher, around 3 mg/m^2 , due to lower absorption sensitivity and given that the chosen spectroscopic retrieval was more sensitive to instrumental noise features.

[10] To obtain the gas emission from a target source, SOF transects, measuring vertically integrated species concentrations, are conducted along roads oriented crosswind and close downwind (0.5–3 km) of the target source so that the detected solar light cuts through the emission plume as illustrated in Figure 2. The gas flux is obtained first by adding the column measurements and hence the integrated mass of the key species across the plume is obtained. To obtain the flux this value is then multiplied by the mass average wind speed of the plume, u'_{mw} . The flux calculation is shown in equation (2). Here, x corresponds to the travel direction, z to the height direction, u' to the wind speed orthogonal to the travel direction (x), u'_{mw} to the mass weighted average wind speed and H_{mix} to the mixing layer height. The slant angle of the Sun is compensated for, by

multiplying the concentration with the cosine factor of the solar zenith angle.

$$flux = \int_{x1}^{x2} \left(\int_0^{H_{mix}} conc(z) \cdot u'(z) \cdot dz \right) dx = u'_{mw} \int_{x1}^{x2} column(x), \quad (2)$$

$$\text{where } u'_{mw} = \frac{\int_0^{H_{mix}} conc(z) u'(z) \cdot dz}{\int_0^{H_{mix}} conc(z) \cdot dz} \text{ and } column = \int_0^{H_{mix}} conc(z) \cdot dz.$$

[11] The determination of the mass averaged wind speed for SOF is not straightforward to obtain as winds are usually complex close to the ground and increase with the height above a surface. What helps the situation is that the measurements can only be undertaken in sunny conditions, which is advantageous since it corresponds to *unstable meteorological conditions* for which wind gradients are smoothed out by convection. Under these conditions the industrial emission plumes mix rather quickly in the vertical giving a more or less homogeneous distribution of the pollutants versus height through the mixing layer even 10 km downwind. In addition to the atmospheric mixing, the plumes from process industries exhibit an initial lift since they are usually hotter than the surrounding air. This assumption of rapid mixing agrees with Doppler LIDAR measurements conducted from the ship RV Ronald H. Brown by NOAA during the TexAQS 2006 [Tucker et al., 2008].

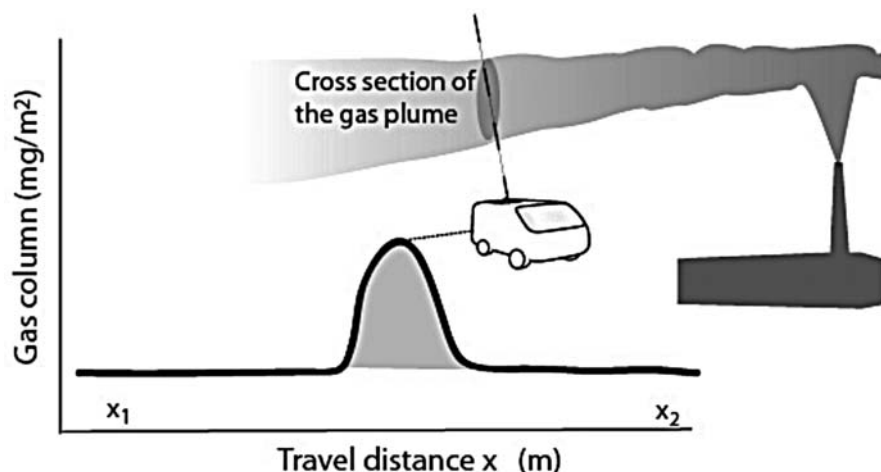


Figure 2. The SOF technique utilizes the absorption of direct solar infrared radiation for retrieval of total columns of various species. The total gas flux emerging from an industrial source is obtained by conducting a downwind transect across its plume and then multiplying the integrated concentration by the plume wind speed.

From these measurements information about mixing height and the vertical mixing of the atmosphere could be obtained showing typical daytime vertical mixing speeds of $\pm(0.5\text{--}1.5)$ m/s.

[12] In the case of the SOF measurements during TexAQS 2006, the measurements were typically conducted at a plume transport time of 200 to 500 s downwind of the industries, which, according to the discussion above, means that sufficient time has elapsed for the emission plume to mix at heights of up to several hundred meters above the ground. For this reason we have used the average wind over the first 200–500 m of the atmosphere as a proxy for the mass weighted wind. Several airborne experiments have been conducted in this study to evaluate the vertical plume mixing and the results are given in section 4.

2.2. Emission Inventories

[13] The measured emissions have been compared to three different emission inventories (EIs). The first is an emission inventory that has been derived by NOAA (G. Frost, unpublished data, 2006) for the state of Texas including emissions of total and selected speciated VOCs and other species from 1858 fixed location pollution sources statewide. The data are based on 2004 annual totals from TCEQ. The 2004 ethylene, propylene and alkane emissions for each point source have been derived from the 2004 total VOC emissions by assuming the same speciation at that point source as in 1999. This inventory will be referred to as the 2004 Annual EI.

[14] The second emission inventory contains hourly emission data for 3192 sources for the time period 15 August to 15 September 2006 (TCEQ, 2006 Point Source Emissions Inventory, accessed October 2008 at <http://www.tceq.state.tx.us/implementation/air/industei/psei/psei.html>) (hereinafter TCEQ data set, 2008). During that period, 141 sites in eastern Texas reported their hourly emissions of VOC based on process flow monitoring (flares, cooling towers) and assumptions about the combustion efficiency of the flare. The sites were selected since they were subject to special

regulation by the TCEQ regarding monitoring and record keeping of their HRVOC emissions. While each source in the 2004 Annual EI corresponds to an entire facility and reports all kinds of emissions from these sources together, this inventory reports each source within a facility and each emitted species from such a source separately. This inventory will be referred to as the 2006 Hourly EI.

[15] The third emission inventory contains daily emission data for 102314 sources for the time period 15 August to 15 October 2006 (TCEQ, data set, 2008). The data are daily averages of the data in the 2006 Hourly Inventory for the sources and time periods for which that data exist and yearly emissions from 2006 for the other sources and time periods. This inventory will be referred to as the 2006 Daily EI. Note that the 2004 Annual EI and the 2006 Daily EI are complete in the sense that they cover all known emission sources at the time while the 2006 Hourly EI is incomplete since it only covers 3192 of the 102314 sources in the 2006 Daily EI.

2.3. Airborne Measurements

[16] In this study the SOF measurements have been compared against airborne ethene measurements by a laser photo acoustic sensor (LPAS) on the NOAA WP-3D airplane [de Gouw *et al.*, 2009]. In addition, comparisons have been made against airborne measurements taken from a Piper Aztec plane from Baylor University [Alvarez *et al.*, 2007] which carried, among other instruments, a chemiluminescence instrument (Thermo Electron 42C) equipped with a molybdenum converter to measure NO_y and a RAD instrument (Rapid Alkene Detector/Hills Scientific) to measure the sum response for several alkenes. The RAD is originally developed for isoprene measurements [Guenther and Hills, 1998], and it is based on the chemiluminescence reaction between alkenes or isoprene and ozone which produces excited formaldehyde emitting light between 450 and 500 nm. The RAD is sensitive to ethene, propene, butadiene and isoprene with a detection limit of around 1 ppb. Response factors relative to propene (volume fraction) for the instrument were measured prior to the campaign yielding

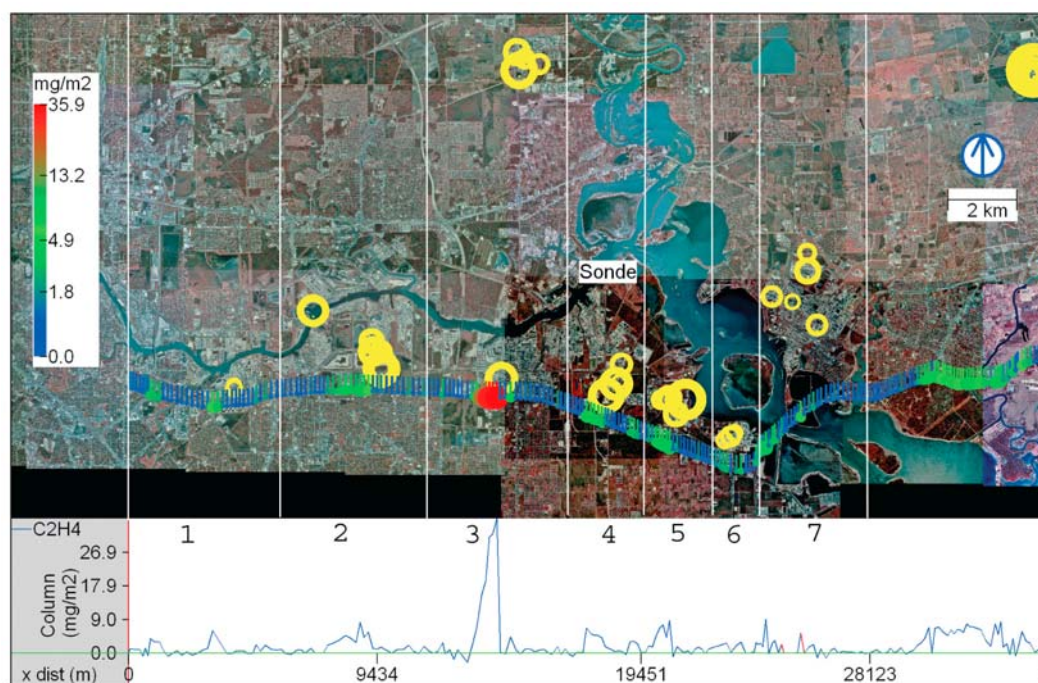


Figure 3. SOF measurement of ethene columns on 30 August 2006 in the HSC. The lines are pointing upwind. The emission rates of the point sources in the Daily 2006 EI are shown in yellow circles with the diameter corresponding to emission rate. The total column values are also shown at the bottom of the plot. Different sectors are shown into which the results have been divided. The location for the GPS sonde measurements is also shown. The accumulated emission in this transects corresponds to 1100 kg/h of ethene.

values of 0.34, 1.39 and 0.92 for ethene, isoprene and 1,3-butadiene, respectively. During the campaign the instrument was regularly calibrated with propene from Scott Specialties, Inc., with an uncertainty of 5%. The RAD alkene values used here have been postcorrected using the ratio between ethene and propene obtained from the SOF measurements.

3. Measurements

[17] During the month of September 2006 SOF measurements were conducted with the aim of pinpointing and quantifying the largest industrial emission sources of VOCs and other species. Six days of measurements were conducted in the vicinity of petrochemical and refinery conglomerates in the HSC area (20 km east of Houston), 1 day in Texas City (50 km SE of Houston), 2 days in Sweeny (90 km SW of Houston) and 1 day in Freeport (85 km south of Houston) and Chocolate Bayou (50 km SSE of Houston). In addition, measurements were conducted at the industrial conglomerate at Bayport, 10 km south of the HSC. The wind direction was northerly to northwesterly during four of the measurement days in the HSC and Mount Belvieu and easterly the other two. For the other sites the wind was south to southwesterly. On a given day, multiple measurements of the emission sources were conducted, if possible both upwind and downwind of the industrial site to capture the enclosed sources and to eliminate background sources. However, since upwind and downwind measurements requires steady state conditions in the solar light and the

wind during several hours, this was only achieved a few times during the campaign for the same day.

[18] A SOF transect conducted on 30 August 2006, measuring columns of ethene across the HSC, is shown in Figure 3. The color-coded circles represent the measured ethene column amounts in mg/m^2 at the specific location. The lines attached to the circles are pointing in the upwind direction. The total column is also shown in the lower part of Figure 3. The known point emissions from the 2006 Daily EI in kg/h are shown as yellow circles, with the diameter corresponding to the emission rate. The measured fluxes in the HSC have been divided into the different sectors shown in Figure 3. The sectors are named: (1) Allen Genoa Rd, (2) Davison Street, (3) Deer Park, (4) Battleground Rd, (5) Miller Cutoff Rd, (6) Sens Rd, and (7) Baytown.

[19] Wind measurements were conducted by launching GPS sondes obtained from Environmental Science Corporation, Boulder. In general three to four soundings were conducted each measurement day. The risetime of the balloons was typically 5 m/s. In the HSC the soundings were carried out close to the Lynchburg Ferry crossing, as shown in Figure 3, in Texas City westward of the town and in Freeport, Chocolate Bayou and Sweeny downwind of the industrial facilities. Wind data was also used from a radar profiler operated by the Texas Commission of Environmental Quality (TCEQ) within the NOAA profiler network at the La Porte Airport south of the HSC (directly south of sector 6). During the TexAQS 2006 campaign TCEQ also operated two SODAR profilers at the Waterworks (middle of sector 1) and the HRM4 (north of sector 3) sites. In addition to the

Table 1. Comparison of Wind Measurements in the Houston Ship Channel^a

| Wind Measurement | Relative Difference From GPS Sonde Wind Speed (0–500 m) (%) | Difference From GPS Sonde Wind Direction (0–500 m) (deg) |
|------------------------------------|--|--|
| Laporte wind profiler (0–500 m) | -3 ± 27 | 2 ± 15 |
| GPS sonde (0–200 m) | -6 ± 15 | 2 ± 9 |
| SODAR waterworks (0–100 m) | -7 ± 24 | 7 ± 16 |
| SODAR HRM4 (0–100 m) | -12 ± 18 | 2 ± 18 |
| Ground stations (CAMS, 10 m) | -29 ± 21 | 12 ± 21 |

^aThe profiler and SODARs correspond to 30 min averages while the GPS sondes travel through the first 500 m layer in 90 s.

wind profilers TCEQ is operating a network of ground stations with wind measurements at 10 m height, which has been used in assessing the wind.

[20] Coordinated measurements with two airplanes, a Piper Aztec from the Baylor University and the NOAA WP-3D, were conducted on several occasions during the project.

[21] The major uncertainty for the SOF measurements lies in the estimation of the mass weighted wind, which includes both uncertainties in plume lift and in the wind profile.

[22] The plume lift has been discussed in section 2.1, and plume lift studies are described in section 4.2. To investigate the wind uncertainty further, various wind measurements during the field campaign were compared to GPS sonde data of the average wind over the first 500 m above ground (see Table 1). This comparison includes measurement errors, systematic spatial wind differences, and differences due to averaging time. It can be seen that all wind speed measurements are within $\pm 30\%$ of each other, except for the ground stations which on average are 30% lower. For the wind direction all measurements are within $\pm 15^\circ$, which corresponds to a 10% flux error in most cases in this study. The wind speed error of 30% and 10% wind direction error are consistent with error estimations conducted in other SOF studies [Kihlman, 2005]. Other sources of error for the SOF measurements include uncertainties in the absorption line parameters of the retrieved compounds and the retrieval uncertainty. The latter is the combined effect of instrumentation and retrieval stability on the retrieved total columns during the course of a plume transect. The composite uncertainty is estimated to be 33% and 38% for ethene and propene, respectively, as seen in Table 2.

4. Results

[23] Measurements of alkenes from various sectors in the HSC, and more isolated sources such as Channelview, Freeport, Mount Belvieu, Sweeny and Texas City are shown here and compared to several emission inventories. The data are also compared to complimentary airborne measurements from which an investigation of the vertical mixing of the industrial plumes has been conducted as well as an independent estimation of the emission rates.

4.1. SOF Measurements

[24] In Table 3 and Table 4 the derived ethene and propene emissions from all individual SOF transects conducted during the campaign are given, together with the geographical coordinates for the studied source regions, the local time of the measurements, wind information and the approximate geographical coordinates for the location of the SOF measurements.

[25] The SOF transect across the HSC shown in Figure 3 was carried out in northerly wind on 30 August between 1100 and 1200 local time (LT), and corresponds to a total flux of 1100 kg/h of ethene and 1850 kg/h of propene. In Figure 3 it can be seen that several sectors in the HSC (3–5) show distinct emission plumes of ethene and that these are downwind of the geographical locations of the emission sources in the Daily 2006 EI, given as yellow circles (a similar picture is seen for propene). In addition in Figure 3, there is an emission plume in the easternmost part of the SOF transect, interpreted as emissions from the far away Mount Belvieu site, shown in the upper right corner of Figure 3. The SOF measurement across the HSC also includes emissions from Channelview, located in the northern part of sector 3. A similar measurement across the HSC later the same day yields an emission rate of 1400 kg/h of ethene while three measurements on 19 September yields an ethene flux of 922 ± 130 kg/h. SOF transects upwind of the Houston Ship Channel in similar meteorological conditions, on highway 10, yield average ethene and propene emissions of 443 kg/h and 488 kg/h, respectively, from Mount Belvieu and 57 kg/h ethene from Channelview (Table 4). Mount Belvieu constitutes the single largest source in the Houston-Galveston area both for ethene and propene. The ethene emission values obtained by SOF agree reasonably well with measurements conducted by NOAA; see below.

[26] In Table 5, the measurement results in Table 3 and Table 4 have been averaged both for ethene and propene. The measured emission values have also been compared to data from the 2006 Daily EI and to the 2004 Annual EI. The EI data has been obtained by, for each SOF transect and sector/region in Table 3 and Table 4, adding all emission sources upwind from the measurement route of each sector, up to a distance of 10 km. The obtained EI data for each transect has then been averaged, in the same way as the SOF data in Table 5. The emission values for a given sector or source region, both for the measurements and the EIs, shows a variability due to the time variation of the emissions but also due to variations in the wind direction which affects which upwind sources that blows into the sectors.

[27] As can be seen in Table 5, the combined emission from the HSC and Mount Belvieu area corresponds to 1250 ± 180 kg/h of ethene and 2140 ± 520 kg/h of propene. This is to be compared to the corresponding 2006 Daily EI values of 145 ± 4 kg/h of ethene and 181 ± 42 kg/h of propene.

Table 2. An Estimated Uncertainty Budget for Flux Measurements With the SOF Method During TexAQS 2006

| | Wind Speed (%) | Wind Direction (%) | Spectroscopy (Cross Sections) (%) | Retrieval (%) | Total Uncertainty (%) |
|---------|----------------------|--------------------------|---|------------------|-----------------------------|
| Ethene | 30 | 10 | 3 | 10 | 33 |
| Propene | 30 | 10 | 3 | 20 | 38 |

Table 3. Ethene and Propene Emissions in the Houston Ship Channel Obtained by SOF Measurements^a

| Emission Source (Latitude/Longitude) | Date | Start–Stop Time (Local Time) | Average Wind (0–500 m Height) GPS Sonde | Ethene (kg/h) | Propene (kg/h) | Approximate Measurement Location |
|---|-------------|---------------------------------|--|------------------|-------------------|-------------------------------------|
| HSC sector 1 | 30 Aug 2006 | 1057–1104 | 6.2 m/s, 359° | 60 | ND | 26.706°N, 95.240°W |
| Allen Genoa Rd | 30 Aug 2006 | 1326–1334 | 6.0 m/s, 001° | 105 | ND | 26.706°N, 95.240°W |
| 29.700°N–29.800°N | 13 Sep 2006 | 1538–1545 | 3.8 m/s, 006° | 111 | ND | 26.706°N, 95.240°W |
| 95.266°W–95.211°W | 19 Sep 2006 | 1025–1032 | 9.4 m/s, 041° | 132 | ND | 26.707°N, 95.250°W |
| | 19 Sep 2006 | 1111–1116 | 9.4 m/s, 041° | 96 | ND | 26.707°N, 95.250°W |
| | 19 Sep 2006 | 1436–1441 | 4.5 m/s, 035° | 52 | ND | 26.707°N, 95.250°W |
| HSC sector 2 | 30 Aug 2006 | 1103–1109 | 6.2 m/s, 359° | 138 | 148 | 29.713°N, 95.189°W |
| Davison Street | 30 Aug 2006 | 1312–1324 | 6.0 m/s, 001° | 170 | NA | 29.713°N, 95.189°W |
| 29.700°N–29.800°N | 13 Sep 2006 | 1523–1528 | 3.8 m/s, 006° | 114 | 115 | 29.713°N, 95.189°W |
| 95.211°W–95.154°W | 19 Sep 2006 | 1018–1024 | 9.4 m/s, 041° | 66 | NA | 29.713°N, 95.194°W |
| | 19 Sep 2006 | 1117–1123 | 9.4 m/s, 041° | 115 | NA | 29.713°N, 95.194°W |
| | 19 Sep 2006 | 1442–1450 | 4.5 m/s, 035° | 146 | 85 | 29.713°N, 95.194°W |
| | 25 Sep 2006 | 1214–1223 | 7.0 m/s, 005° | 100 | 251 | 29.713°N, 95.189°W |
| HSC sector 3 | 30 Aug 2006 | 1111–1115 | 6.2 m/s, 359° | 401 | 710 | 29.711°N, 95.132°W |
| Deer Park | 30 Aug 2006 | 1301–1307 | 6.0 m/s, 001° | 279 | 895 | 29.711°N, 95.132°W |
| 29.700°N–29.800°N | 13 Sep 2006 | 1509–1515 | 3.8 m/s, 006° | 105 | 246 | 29.711°N, 95.132°W |
| 95.154°W–95.103°W | 19 Sep 2006 | 1006–1015 | 9.4 m/s, 041° | 223 | NA | 29.711°N, 95.136°W |
| | 19 Sep 2006 | 1126–1131 | 9.4 m/s, 041° | 67 | 144 | 29.711°N, 95.136°W |
| | 19 Sep 2006 | 1451–1458 | 4.5 m/s, 035° | 71 | 17 | 29.711°N, 95.136°W |
| | 25 Sep 2006 | 1205–1211 | 7.0 m/s, 005° | 183 | 140 | 29.711°N, 95.132°W |
| HSC sector 4 | 30 Aug 2006 | 1117–1120 | 6.2 m/s, 359° | 74 | 144 | 29.704°N, 95.093°W |
| Battleground Rd | 13 Sep 2006 | 1501–1506 | 3.8 m/s, 006° | 158 | 1010 | 29.704°N, 95.093°W |
| 29.700°N–29.750°N | 19 Sep 2006 | 1001–1004 | 9.4 m/s, 041° | 120 | NA | 29.706°N, 95.096°W |
| 95.103°W–95.084°W | 19 Sep 2006 | 1139–1141 | 9.4 m/s, 041° | 56 | NA | 29.706°N, 95.096°W |
| | 19 Sep 2006 | 1457–1503 | 4.5 m/s, 035° | NA | 214 | 29.706°N, 95.096°W |
| | 25 Sep 2006 | 1154–1157 | 7.0 m/s, 005° | 49 | 185 | 29.704°N, 95.093°W |
| HSC sector 5 | 30 Aug 2006 | 1119–1124 | 6.2 m/s, 359° | 115 | 289 | 29.697°N, 95.067°W |
| Miller Cutoff Rd | 30 Aug 2006 | 1247–1250 | 6.0 m/s, 001° | NA | 235 | 29.697°N, 95.067°W |
| 29.695°N–29.750°N | 13 Sep 2006 | 1455–1501 | 3.8 m/s, 006° | 363 | 235 | 29.697°N, 95.067°W |
| 95.084°W–95.054°W | 25 Sep 2006 | 1149–1154 | 7.0 m/s, 005° | 75 | 158 | 29.697°N, 95.067°W |
| HSC sector 6 | 30 Aug 2006 | 1123–1127 | 6.2 m/s, 359° | 52 | 227 | 29.688°N, 95.039°W |
| Sens Rd | | | | | | |
| 29.685°N–29.710°N | | | | | | |
| 95.054°W–95.030°W | | | | | | |
| HSC sector 7 | 30 Aug 2006 | 1127–1135 | 6.2 m/s, 359° | 70 | 358 | 29.707°N, 95.012°W |
| Baytown | 7 Sep 2006 | 1222–1236 | 2.0 m/s, 075° | 47 | 177 | 29.736°N, 95.023°W |
| 29.706°N–29.780°N | 13 Sep 2006 | 1449–1454 | 4.6 m/s, 010° | 104 | NA | 29.710°N, 95.007°W |
| 95.030°W–94.981°W | 25 Sep 2006 | 1120–1126 | 7.0 m/s, 005° | 68 | 362 | 29.736°N, 95.023°W |

^aND, not detected; NA, not available.

[28] For ethene the typical discrepancy factors, calculated as a geometric mean, between SOF and the 2006 daily and 2004 annual EIs are 10.2(+8,-5) and 17.4(+18,-9), respectively (geometric standard deviation in brackets). For propene the corresponding discrepancy factors are 11.7(+7,-4) and 16.0(+15,-8). The geometric mean (logarithmic average) is used since we are averaging ratios, and this average is smaller than the arithmetic one. Note that some emission values in Table 5 are based on only one transect, making these measurements uncertain.

[29] For the measurements conducted in the HSC with northerly wind, Table 3, the largest temporal variability in the emissions was seen in propene for the sectors 3 and 4, with 93% variability, while for ethene the highest variability was seen for the sectors 3 and 5, with 60–70% variability. A more detailed study of temporal variability was also carried out by conducting north-south transects in the middle of sector 4 in an easterly wind, thus measuring the combined emissions from sectors 4–6, and possibly also sector 7 (Table 4). In Figure 4, such a SOF measurement of

propene is shown on 31 August at noon time when conducting a southward transect on Battleground Rd, sector 4, with an easterly wind. The emission sources in the 2006 daily EI are also indicated. The emission values from the SOF measurement were high in this transect, i.e., 2295 kg/h, compared to what was measured 30 min prior to, i.e., 684 kg/h, and after, i.e., 237 kg/h, this occasion. All in all, six transects of the sectors 4–6, in both easterly and northerly wind were carried out over 4 days. In Figure 5, these data have been plotted versus time together with the corresponding data from various EIs for the period 15 August to 15 September. It can be seen that there are generally large emission variations on small time scales over the whole month in this region, including some really high and sharp peaks. However, none of these variations overlapped with the SOF measurements, although it was very close for the ones conducted on 13 and 14 September. Hence, in the region east of Battleground Rd, there are emission sources that according to the 2006 hourly EI can vary by an order of magnitude or more and possibly cause the observed vari-

Table 4. Ethene and Propene Emissions From Various Isolated Sources in Southeast Texas and the Eastern Part of the Houston Ship Channel Obtained by SOF Measurements^a

| Source Region Latitude/ Longitude Borders | Date | Local Time | Average Wind (0–500 m Height) GPS Sonde | Ethene (kg/h) | Propene (kg/h) | Approximate Measurement Location |
|--|---|---|--|--|--|--|
| Bayport 29.662°N–29.665°N 95.096°W–95.032°W | 26 Sep 2006 | 1054–1109 | 2.3 m/s, 038° | 163 | ND | 29.622°N, 95.096°W |
| Channelview 29.810°N–29.838°N 95.125°W–95.101°W | 31 Aug 2006 31 Aug 2006 19 Sep 2006 26 Sep 2006 | 1648–1703 1757–1813 1355–1408 1515–1529 | 3.0 m/s, 043° 2.0 m/s, 126° 6.0 m/s, 032° 2.8 m/s, 051° | 46.268 22.751 60.682 97.924 | ND ND ND ND | 29.823°N, 95.127°W 29.823°N, 95.127°W 29.770°N, 95.182°W 29.820°N, 95.127°W |
| Chocolate Bayou 29.240°N–29.260°N 95.228°W–95.204°W | 27 Sep 2006 | 1027–1049 | 4.1 m/s, 184° | 136 | 273 | 29.268°N, 95.190°W |
| Freeport 28.940°N–29.260°N 95.228°W–95.204°W | 27 Sep 2006 27 Sep 2006 27 Sep 2006 | 1237–1252 1302–1344 1417–1425 | 4.0 m/s, 183° 4.0 m/s, 183° 5.0 m/s, 200° | 215 325 211 | ND ND ND | 29.007°N, 95.397°W 29.007°N, 95.397°W 29.007°N, 95.397°W |
| Mount Belvieu 29.820°N–29.883°N 94.941°W–94.878°W | 30 Aug 2006 30 Aug 2006 19 Sep 2006 25 Sep 2006 25 Sep 2006 25 Sep 2006 | 1132–1142 1216–1229 1311–1333 1456–1524 1555–1606 1643–1701 | 6.2 m/s, 359° 6.0 m/s, 001° 6.0 m/s, 032° 6.6 m/s, 353° 6.6 m/s, 353° 6.6 m/s, 353° | 354 275 331 559 536 605 | NA NA 222 NA 646 596 | 29.719°N, 94.947°W 29.727°N, 94.909°W 29.810°N, 94.950°W 29.820°N, 94.912°W 29.820°N, 94.912°W 29.820°N, 94.912°W |
| Sweeny 29.062°N–29.084°N 95.761°W–95.731°W | 21 Sep 2006 21 Sep 2006 21 Sep 2006 27 Sep 2006 27 Sep 2006 27 Sep 2006 27 Sep 2006 | 1148–1154 1156–1201 1445–1502 1616–1622 1643–1651 1708–1716 1726–1750 | 10.0 m/s, 191° 10.0 m/s, 191° 10.0 m/s, 191° 2.2 m/s, 185° 2.2 m/s, 185° 2.2 m/s, 185° 2.2 m/s, 185° | 55 174 273 136 124 186 192 | NA NA NA NA 79 200 101 | 29.079°N, 95.750°W 29.079°N, 95.750°W 29.079°N, 95.750°W 29.079°N, 95.750°W 29.079°N, 95.750°W 29.079°N, 95.750°W 29.079°N, 95.750°W |
| Texas City 29.354°N–29.384°N 94.949°W–94.888°W | 20 Sep 2006 20 Sep 2006 20 Sep 2006 | 0929–0939 1208–1215 1228–1235 | 3.8 m/s, 060° 3.8 m/s, 060° 3.8 m/s, 060° | 80 72 95 | ND ND ND | 29.363°N, 94.947°W 29.363°N, 94.947°W 29.363°N, 94.947°W |
| HSC east Sector 4–6 29.690°N–29.740°N 95.090°W–95.032°W | 31 Aug 2006 31 Aug 2006 31 Aug 2006 31 Aug 2006 14 Sep 2006 14 Sep 2006 14 Sep 2006 | 1054–1112 1150–1209 1219–1234 1252–1310 1435–1500 1537–1603 1608–1636 | 2.3 m/s, 075° 2.3 m/s, 075° 2.3 m/s, 075° 2.3 m/s, 075° 5.6 m/s, 107° 4.0 m/s, 120° 4.0 m/s, 120° | 158.82 254.28 276.42 95.139 479.82 264.92 437.32 | NA 683.61 2294.6 237.47 1319.8 NA NA | 29.723°N, 95.089°W 29.723°N, 95.089°W 29.723°N, 95.089°W 29.723°N, 95.089°W 29.723°N, 95.089°W 29.723°N, 95.089°W 29.723°N, 95.089°W |

^aND, not detected; NA, not available.

ability on 31 August. Even though there are 21 propene sources in this area in the hourly EI, all the large fluctuations seen in Figure 5 are dominated by emissions from four flares, marked with red circles in Figure 4. Noteworthy is that the high propene flux measured by SOF in Figure 4 was located just downwind of these four flares. Similar measurements were also conducted in sector 3 with the same type of results.

[30] In Figure 6, SOF measurements are shown at the isolated source in Sweeny on 27 September together with 2006 daily EI data. The average emission for three measurements on this day for ethene and propene corresponds to 160 ± 34 kg/h and 127 ± 65 kg/h, respectively. This can be compared to the 2006 Daily EI values of 10 and 8 kg/h for ethene and propene, respectively. The GPS wind measurement was conducted just north of the facility. Airborne measurements were conducted in parallel here to investigate the plume lift, as described below.

4.2. Complementary Airborne Measurements

[31] Measurements of ethene at Mount Belvieu, sector 8, by the NOAA WP-3D during September of 2006 shows an average emission of 520 kg/h with an uncertainty of 50%, based on 10 transects between 13 September and 13 October [de Gouw *et al.*, 2009]. This can be compared with the average SOF value from Table 5 of 443 kg/h with an uncertainty of 35%, based on 6 transects (31 August, 13 September and 25 September). The 2006 daily EI shows an emission value of 81 kg/h here. The emissions from the WP-3D were obtained by measuring the mixing ratio of ethene at distances corresponding to 1000–2000 s transport time of the plume downwind of the industry, at several flight altitudes. It was then assumed that the gas plume was well mixed through the whole mixing layer and this made it possible to calculate gas columns from the measured mixing ratio data. These columns, integrated across the plume, were then converted to a gas flux by multiplication with the wind speed, in a similar fashion to the SOF method.

Table 5. Average Ethene and Propene Emissions Obtained by SOF Measurements and Emission Inventories for September 2006^a

| Source Region | Species | SOF 2006 (kg/h) | 2006 Daily Inventory (kg/h) | 2004 Annual Inventory (kg/h) | Number of Measurements |
|------------------------|---------|--------------------|--------------------------------|---------------------------------|---------------------------|
| HSC sector 1: | Ethene | 93 ± 28 | 5.2 ± 1.1 | 1.5 ± 0.3 | 6 |
| Allen Genoa Rd | Propene | ND | | | |
| HSC sector 2: | Ethene | 122 ± 31 | 12.8 ± 2.4 | 8.0 ± 1.2 | 7 |
| Davison Street | Propene | 150 ± 62 | 8.9 ± 4.3 | 8.1 ± 0.9 | 4 |
| HSC sector 3: | Ethene | 190 ± 113 | 4.7 ± 0.5 | 3.8 ± 0.6 | 7 |
| Deer Park | Propene | 359 ± 325 | 13.0 ± 2.0 | 8.14 ± 0.9 | 6 |
| HSC sector 4: | Ethene | 91 ± 41 | 13.3 ± 0.9 | 3.6 ± 2.1 | 5 |
| Battleground Rd | Propene | 388 ± 360 | 62.6 ± 21.1 | 20.3 ± 5.9 | 4 |
| HSC sector 5: | Ethene | 184 ± 127 | 15.7 ± 6.9 | 29.6 ± 0.8 | 3 |
| Miller Cutoff Rd | Propene | 229 ± 47 | 29.5 ± 36.6 | 10.7 ± 5.0 | 4 |
| HSC sector 6: | Ethene | 52 | 2.8 | 3.3 | 1 |
| Sens Rd | Propene | 227 | 0 | 0 | 1 |
| HSC sector 7: | Ethene | 72 ± 21 | 9.4 ± 1.2 | 6.5 ± 0.2 | 4 |
| Baytown | Propene | 300 ± 86 | 23.7 ± 4.3 | 35.3 ± 11.3 | 3 |
| Total HSC ^b | Ethene | 804 ± 127 | 64 ± 3.0 | 56 ± 0.2 | |
| | Propene | 1653 ± 490 | 138 ± 43 | 82 ± 11 | |
| Bayport | Ethene | 163 | 22.4 | 6.8 | 1 |
| | Propene | ND | 13.2 | 10.8 | 1 |
| Channelview | Ethene | 57 ± 27 | 7.3 ± 0.2 | 11.8 ± 0.1 | 4 |
| | Propene | ND | | | |
| Chocolate Bayou | Ethene | 136 | 42.1 | 10.0 | 1 |
| | Propene | 273 | 29.3 | 24.7 | 1 |
| Freeport | Ethene | 250 ± 53 | 39.0 ± 1.9 | 7.0 ± 10.0 | 3 |
| | Propene | ND | | | |
| Mount Belvieu | Ethene | 443 ± 127 | 81.1 ± 1.8 | 44.8 ± 0.0 | 6 |
| | Propene | 488 ± 189 | 35.0 ± 3.2 | 12.2 ± 1.0 | 3 |
| Sweeny | Ethene | 163 ± 63 | 10.0 ± 0.2 | 4.8 ± 0.0 | 7 |
| | Propene | 127 ± 53 | 7.4 ± 0.2 | 5.1 ± 0.0 | 3 |
| Texas City | Ethene | 83 ± 9 | 7.0 ± 0.0 | 8.6 ± 0.0 | 3 |
| | Propene | ND | 8.7 ± 0.0 | 10.7 ± 0.0 | 3 |

^aThe given variability is not the uncertainty but corresponds to the variations of the emissions and variations in which sources blows in to the sectors due to the wind direction. The sectors in the HSC were measured in northerly wind. ND, not detected.

^bIncludes Channelview.

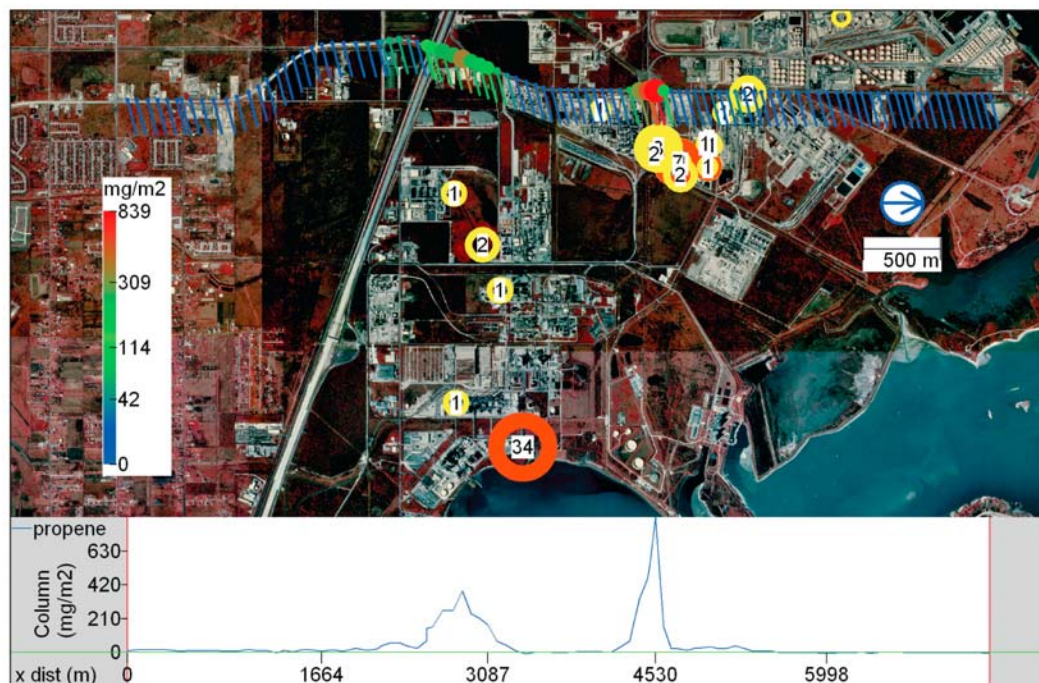


Figure 4. SOF measurement of propene columns on 31 August 2006 when conducting a southward transect on Battleground Rd. North is to the right. The emission rates of the point sources in the Daily 2006 EI in kg/h are shown in yellow circles and the dominant ones are shown in red. The total column values are also shown at the bottom of the plot.

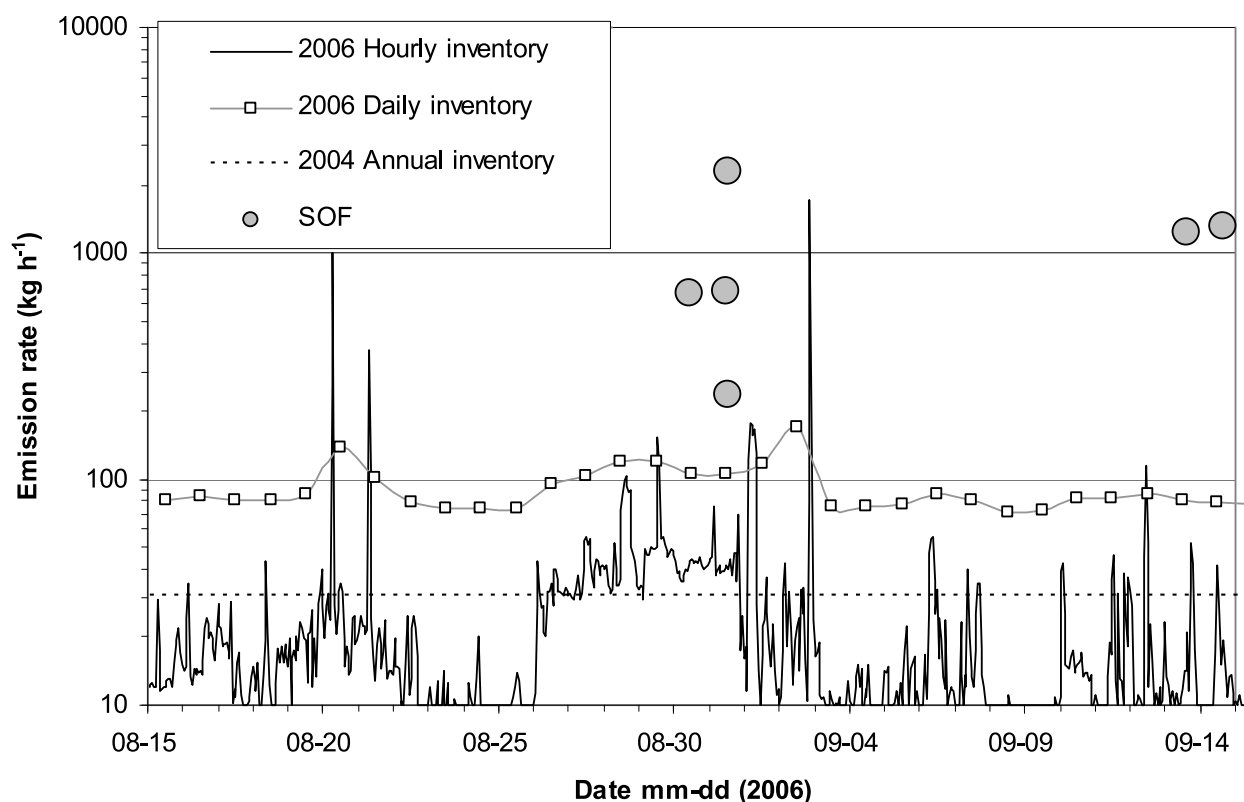


Figure 5. Time plots of total propene emissions from the sources east of Battleground Rd (areas 4–6) according to several emission inventories and SOF measurements.

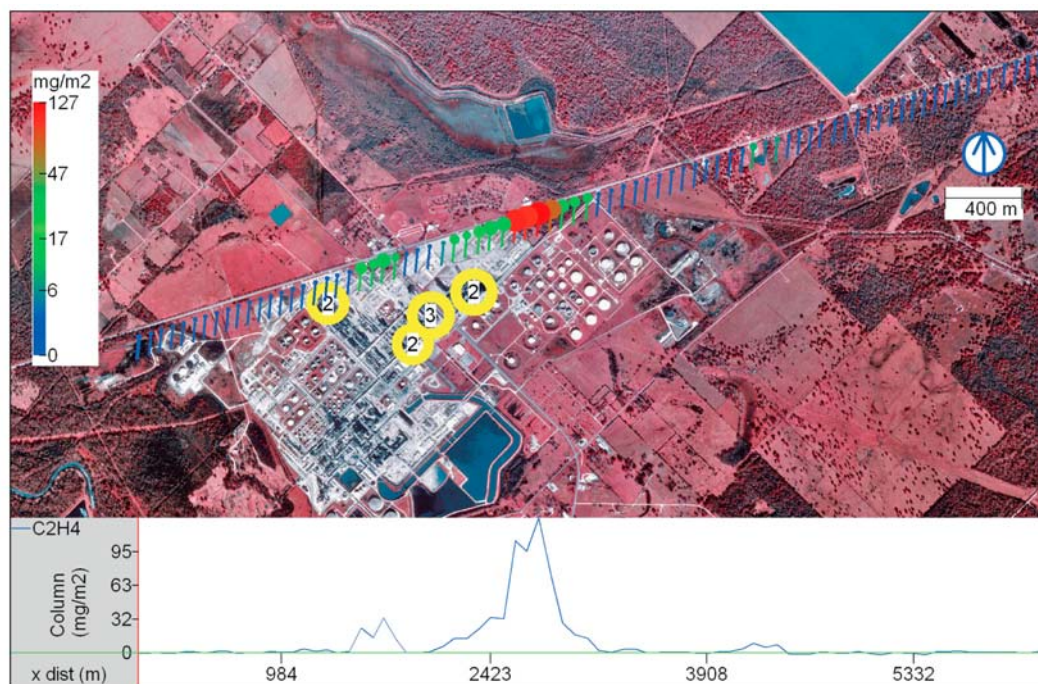


Figure 6. SOF measurement of ethene columns at Sweeny on 27 September 2006. The lines are pointing upwind. The emission rates of the point sources in the Daily 2006 EI in kg/h are shown in yellow circles. The total column values are also shown at the bottom of the plot.

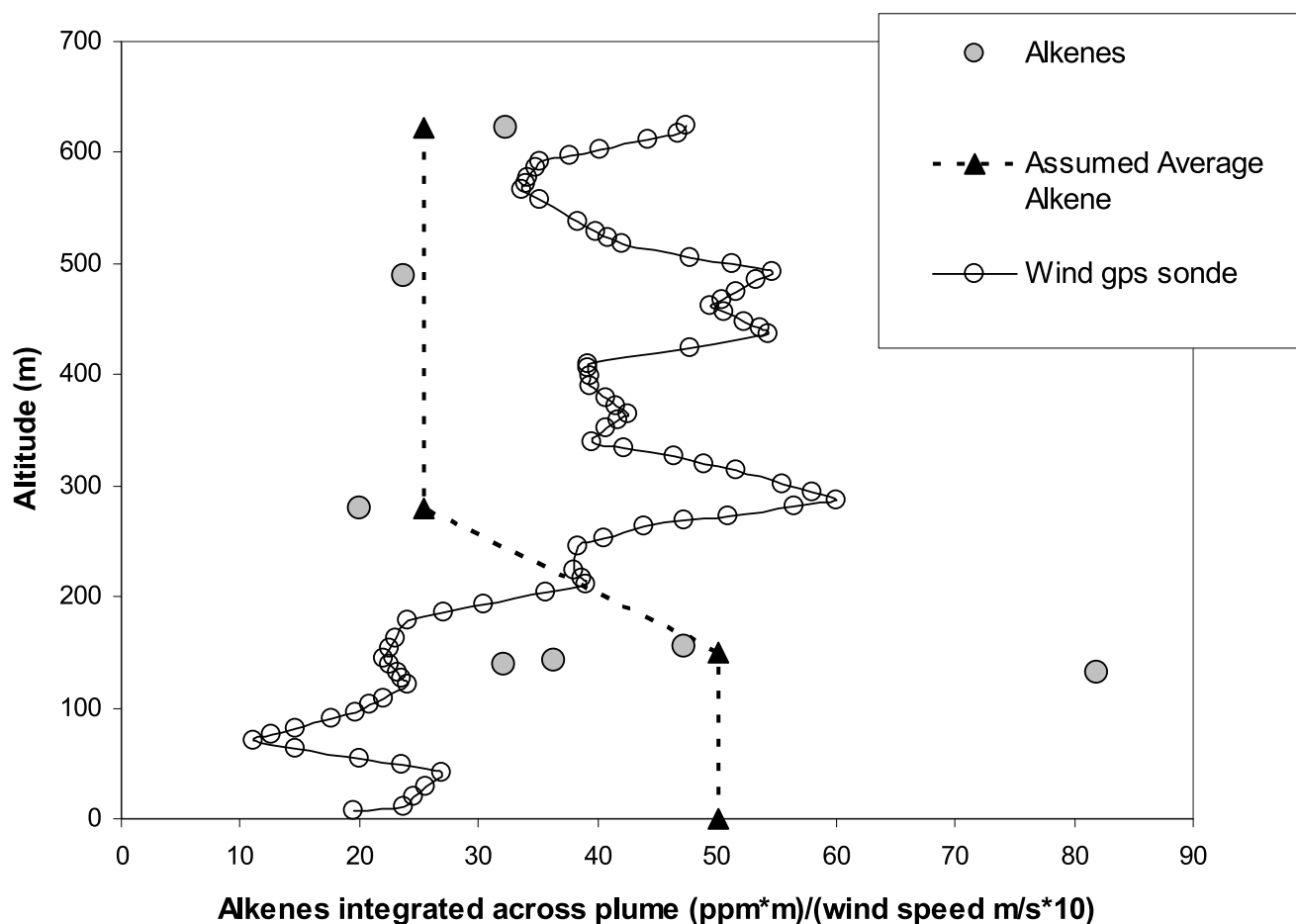


Figure 7. Measurement of alkenes with the Baylor Piper Aztec. The horizontally integrated concentration values across the plume are shown with gray circles. In addition the wind profile measured by the GPS sounding and the assumed average alkene profile are shown.

[32] The Piper Aztec from Baylor University flew above the SOF path on several occasions. On 27 September measurements were conducted at several heights close to the industrial facility in Sweeny along the SOF path shown in Figure 6. In Figure 7 the horizontally integrated concentration values of alkenes (ppm-m) from the airborne RAD instrument are shown as gray circles, across the plume versus height. In addition the wind profile measured by the GPS sounding just north of the facility is shown. The RAD values have been post corrected by a factor of 1.76 by assuming a number ratio between ethene and propene of 1.9 in the plume as measured by the SOF instrument during the same time and taking into account the response factors of the two species. It is estimated that the measurements were taken at a distance from the source which corresponds to 250 s transport time downwind of the plume. It can be seen that the highest average value is found at 150 m altitude, although there is quite a large variability, and that the average value is 50% lower at the higher altitudes up to at least 600 m. The large variability at the lower altitude is probably caused by the fact that the plume is rather turbulent at this height. The 50% lower values at the higher altitudes are consistent with the fact that the wind speed is higher above 150 m and that it is diluting the concentration more there. It thus seems that the plume is mixed evenly up

to at least 600 m, and this indicates a 2.5 m/s vertical mixing speed since the plume traveling time is 250 s. This value is surprisingly high, compared to the vertical wind measurement of 0.5–1 m/s conducted by the Doppler LIDAR already mentioned in section 2. From the mixing ratio data in Figure 7 a rough mixing ratio profile has been derived by calculating the average mixing ratio of the lower altitudes and then the average of the upper altitude values and then assuming zero values above 600 m. Assuming this profile to be correct it is possible to calculate the true mass weighted wind speed, according to equation (2) which should be used for the SOF measurements, and in this case it corresponds to 3.3 m/s. This should be compared to the average wind value over the first 200 m, i.e., 2.2 m/s, applied in the SOF measurement and which yields a flux value that is 33% lower than the mass weighted wind speed.

[33] Similar measurements to the one in Sweeny were made by the Baylor Piper Aztec airplane at the nearby Freeport industrial facility with similar results; the VOCs in the plume mixed all the way up to 500 m, at a plume travel time of about 250 s downwind of the source. Measurements were also conducted at Texas City with a plume rising to about 300 m, but here it is uncertain how far away the sources were.

[34] The flux from the average mixing ratio profile in Figure 7 can be obtained by multiplying the concentration with the wind speed at each height in the same manner as in the SOF approach. An alkene flux of 450 kg/h is obtained, which should be compared with the SOF estimate of the alkene emission for this day of 287 kg/h. It is also possible to calculate the emissions from the Sweeny facility in an indirect way by calculating the average mass ratio of alkenes to NO_y in the plume from the airborne data and then multiplying with the reported emission rate of NO_x for the facility [Ryerson *et al.*, 2003]. This assumes that the latter value is better understood than the alkene emission. Here, an alkene to NO_y ratio of 1.4 was obtained by taking the ratio of the sum of all alkenes from the RAD instrument and the sum of all NO_y , obtained by chemiluminescence. The emission rate of NO_x reported for Sweeny in the 2006 daily EI is 292 kg/h, and thus this implies that the emission of alkenes corresponds to 397 kg/h, obtained through multiplication with the measured alkene to NO_x ratio.

[35] Another parallel measurement between SOF and the Baylor Piper Aztec was conducted at the industrial site in Chocolate Bayou. Here the SOF measurements, Table 5 show that 368 kg/h of alkenes are being emitted, to be compared to 530 kg/h obtained from the airborne measurements using the ratio between alkenes, measured by RAD and NO_y and the 2006 daily EI value of NO_x .

5. Discussion and Conclusion

[36] The results from the campaign that was carried out during September 2006 in the Houston area, show that the emissions of ethene and propene, obtained by SOF, are on average an order of magnitude larger than what is reported in the 2006 daily EI. The largest single emission source of HRVOCs in the vicinity of Houston was the Mount Belvieu area with emissions that are 5 and 12 times higher for ethene and propene, respectively, than reported in the 2006 daily EI.

[37] In some sectors in the HSC, large variability in the alkene emissions, especially propene, was observed downwind of petrochemical plants. There is poor correlation between these measurements and the emission rates reported in the 2006 hourly EI, but the same plants in general report highly variable flare emissions during August and September 2006, which actually dominate their total emissions of alkenes from time to time.

[38] As described in section 2.2 the reported emissions for flares are based on monitoring of the mass flow to the flares. The hourly emission inventory developed from this data assumes a fixed combustion efficiency of 98–99%, corresponding to the permitting guidance for flares. As shown in this work this current approach does not match observations.

[39] Even though there is poor correlation between the measurement and the EI, we believe it is still likely that the variable and large emissions measured by SOF are caused by flaring, since these were measured just downwind of the flares, i.e., coincide geographically, and due to their large temporal variation, which is consistent with flaring events. This is consistent with the fact that large alkene emissions from petrochemical flares have been observed in another Swedish SOF study [Mellqvist, 2001].

[40] The estimated uncertainty for the SOF measurements is about 35%, based on the measured variability in the wind during the campaign, i.e., 30%, and assumptions about vertical mixing, i.e., that the plume mixes vertically with a speed of 0.5–1 m/s. As discussed in section 2.1 the vertical wind speed is supported by the NOAA Doppler LIDAR measurements. It is further supported by airborne measurements by the Baylor Piper Aztec in Sweeny and Freeport, showing that the alkene plume was distributed up to 600 m, even at a plume transport time of 250 s downwind of the plume. It is unlikely that this strong plume raise is all due to normal vertical mixing due to convection of the air, since this would correspond to a vertical mixing speed of more than 2 m/s. It may instead, partly, be caused by initial plume lift due to the fact that air inside the industrial process is hotter than the surrounding air, and this may explain the strong vertical mixing observed.

[41] Airborne and SOF measurements of alkene emissions were compared at three sites. For measurements at Mount Belvieu, the NOAA WP-3D shows 17% higher emission values on average than the SOF measurements during the campaign, but for a single simultaneous measurement on 25 September the NOAA WP-3D shows a 60% higher value. Measurements at Sweeny on 27 September by the Baylor Piper Aztec show emissions that were 45–55% higher than the SOF measurement. Here two approaches were used to obtain the flux, either by using the ratio of alkenes to NO_x and then multiplying with the reported NO_x emissions and the other based on using the concentration and mass profile in Figure 7.

[42] Similar measurements at Chocolate Bayou on 27 September show an alkene emission from the airplane which is 47% higher than the one obtained by the SOF method. Here the airborne emission was obtained through the ratio of alkenes to NO_y which was then multiplied with the reported NO_x emission. The SOF measurement here is rather uncertain since only one transect was conducted.

[43] Hence, in general the comparison between SOF and airborne measurements shows an agreement within 50%. Even though several examples show that the SOF method is consistently lower this is probably a coincidence and we actually believe that most of the discrepancy is caused by uncertainties in the airborne estimations. For instance the ratio method is dependent on accurate NO_x emissions in the inventory and assumes good mixing between the NO_x and alkenes. This is not entirely true, as already discussed in section 1. The method applied by NOAA [de Gouw *et al.*, 2009] has an estimated uncertainty of 50% and is dependent on full mixing in the mixing layer and that the mixing layer height is known. Nevertheless, even though there is 17–50% discrepancy between the SOF and airborne methods, this uncertainty has to be put into context with the 900% discrepancy between the SOF measurements and the emission inventories.

[44] **Acknowledgments.** The SOF measurements and analysis were funded by Texas Environmental Research Consortium (TERC) under project H53. Further analysis has also been funded by TCEQ under contract 582-5-64594-FY08-06. The authors would like to thank Elisabeth Undén for assisting with the SOF measurements and Monica Patel and Craig Clements for conducting the GPS soundings. We thank TNRIS for providing digital maps and TCEQ for supplying auto-GC and wind profiler

data. The Baylor Piper Aztec data was funded by TERC under project H63. We thank Levi Kauffman, Tim Compton, Grazia Zanin, Maxwell Shauck, and Martin Buhr for conducting part of the work with the Piper Aztec, and Noor Gillani is acknowledged for flight planning. Joost de Gouw is acknowledged for providing LPAS data.

References

- Alvarez, S., et al. (2007), H-63 Aircraft Measurements in support of TexAQS II, report, Tex. Environ. Res. Consortium, Houston.
- Burton, M. R., C. Oppenheimer, L. A. Horrocks, and P. W. Francis (2001), Diurnal changes in volcanic plume chemistry observed by lunar and solar occultation spectroscopy, *Geophys. Res. Lett.*, **28**, 843–846, doi:10.1029/2000GL008499.
- de Gouw, J. A., et al. (2009), Airborne measurements of ethene from industrial sources using laser photo-acoustic spectroscopy, *Environ. Sci. Technol.*, **43**, 2437–2442, doi:10.1021/es802701a.
- Foy, B., et al. (2007), Modelling constraints on the emission inventory and on vertical dispersion for CO and SO₂ in the Mexico City metropolitan area using solar FTIR and zenith sky UV spectroscopy, *Atmos. Chem. Phys.*, **7**, 781–801.
- Galle, B., et al. (1999), Ground Based FTIR Measurements of Stratospheric Trace Species from Harestua, Norway during Sesame and Comparison with a 3-D Model, *J. Atmos. Chem.*, **32**(1), 147–164, doi:10.1023/A:1006137924562.
- Galle, B., C. Oppenheimer, A. Geyer, A. McGonigle, and M. Edmonds (2003), A miniaturised ultraviolet spectrometer for remote sensing of SO₂ fluxes: A new tool for volcano surveillance, *J. Volcanol.*, **119**, 241–254, doi:10.1016/S0377-0273(02)00356-6.
- Griffith, D. W. T. (1996), Synthetic calibration and quantitative analysis of gas-phase FT-IR spectra, *Appl. Spectrosc.*, **50**(1), 59–70, doi:10.1366/0003702963906627.
- Guenther, A. B., and A. J. Hills (1998), Eddy covariance measurement of isoprene fluxes, *J. Geophys. Res.*, **103**(D11), 13,145–13,152, doi:10.1029/97JD03283.
- Hanst, P. L., et al. (1982), A long path infrared study of Los Angeles smog, *Atmos. Environ.*, **16**, 969–981, doi:10.1016/0004-6981(82)90183-4.
- Kihlman, M. (2005), Application of solar FTIR spectroscopy for quantifying gas emissions, *Tech. Rep. 4*, Dep. of Radio and Space Sci., Chalmers Univ. of Technol., Gothenburg, Sweden.
- Kihlman, M., J. Mellqvist, and J. Samuelsson (2005), Monitoring of VOC emissions from three refineries in Sweden and the Oil Harbour of Göteborg using the solar occultation flux method, technical report, Dep. of Radio and Space Sci., Chalmers Univ. of Technol., Gothenburg, Sweden.
- Mellqvist, J. (1999), Application of infrared and UV-visible remote sensing techniques for studying the stratosphere and for estimating anthropogenic emissions, Ph.D. thesis, Chalmers Univ. of Technol., Göteborg, Sweden.
- Mellqvist, J. (2001), Flare testing using the SOF method at Borealis polyethene in the summer of 2000, report, Chalmers Univ. of Technol., Gothenburg, Sweden.
- Mellqvist, J., B. Galle, T. Blumenstock, F. Hase, D. Yashcov, J. Notholt, B. Sen, J.-F. Blavier, G. C. Toon, and M. P. Chipperfield (2002), Ground-based FTIR observations of chlorine activation and ozone depletion inside the Arctic vortex during the winter of 1999/2000, *J. Geophys. Res.*, **107**(D20), 8263, doi:10.1029/2001JD001080.
- Mellqvist, J., B. Galle, J. Samuelsson, and A. Strandberg (2004), Mobile column measurements of CO in megacities, in *Proceedings of The XVIII Quadrennial Ozone Symposium*, edited by C. Zerefos, pp. 612–613, Int. Ozone Comm., Halkidiki, Greece.
- Mellqvist, J., et al. (2005), Mobile solar FTIR Measurements of SO₂, HCl and HF in the gas plumes of active volcanoes, paper presented at 9th Gas Workshop, Comm. on the Chem. of Volcanic Gases, Int. Assoc. of Volcanol. and Chem. of the Earth's Int., Palermo, Italy.
- Mellqvist, J., J. Samuelsson, C. Rivera, B. Lefer, and M. Patel (2007), Measurements of industrial emissions of VOCs, NH₃, NO₂ and SO₂ in Texas using the solar occultation flux method and mobile DOAS, report, Texas Environ. Res. Consortium, Houston.
- Mellqvist, J., J. Samuelsson, C. Rivera, B. Lefer, M. Patel, and S. Alvarez (2008), Comparison of solar occultation flux measurements to the 2006 TCEQ emission inventory and airborne measurements for the TexAQS II, report, Tex. Comm. on Environ. Qual., Austin, Tex.
- Rinsland, C. P., R. Zander, and P. Demoulin (1991), Ground-based infrared measurements of HNO₃ total column abundances: Long-term trend and variability, *J. Geophys. Res.*, **96**(D5), 9379–9389, doi:10.1029/91JD00609.
- Rivera, C., J. Mellqvist, J. Samuelsson, B. Lefer, S. Alvarez, and M. Patel (2010), Quantification of NO₂ and SO₂ emissions from the Houston Ship Channel and Texas City industrial areas during the 2006 Texas Air Quality Study, *J. Geophys. Res.*, doi:10.1029/2009JD012675, in press.
- Rothman, L. S., et al. (2005), HITRAN 2004 molecular spectroscopic database, *J. Quant. Spectrosc. Radiat. Transfer*, **96**, 139–204, doi:10.1016/j.jqsrt.2004.10.008.
- Ryerson, T. B., et al. (2003), Effect of petrochemical industrial emissions of reactive alkenes and NO_x on tropospheric ozone formation in Houston, Texas, *J. Geophys. Res.*, **108**(D8), 4249, doi:10.1029/2002JD003070.
- Sharpe, S., et al. (2004), Gas-phase databases for quantitative infrared spectroscopy, *Appl. Opt.*, **58**(12), 1452–1461.
- Tucker, S., et al. (2008), Doppler lidar estimation of mixing height using turbulence, shear, and aerosol profiles, *J. Atmos. Oceanic Technol.*, **26**(4), 673–688, doi:10.1175/2008JTECHA1157.1.
- Walmsley, H. L., and S. J. O'Connor (1998), The accuracy and sensitivity of infrared differential absorption lidar measurements of hydrocarbon emissions from process units, *Pure Appl. Opt.*, **7**, 907–925, doi:10.1088/0963-9659/7/4/024.
- Weibring, P., et al. (1998), Monitoring of volcanic sulphur dioxide emissions using differential absorption lidar (DIAL), differential optical absorption spectroscopy (DOAS), and correlation spectroscopy (COSPEC), *Appl. Phys. B*, **67**, 419–426, doi:10.1007/s003400050525.
- Wert, B. P., et al. (2003), Signatures of terminal alkene oxidation in airborne formaldehyde measurements during TexAQS 2000, *J. Geophys. Res.*, **108**(D3), 4104, doi:10.1029/2002JD002502.
- S. Alvarez, Institute for Air Science, Baylor University, Waco, TX 76798, USA.
- J. Johansson, J. Mellqvist, C. Rivera, and J. Samuelsson, Radio and Space Science, Chalmers University of Technology, Horsalsvagen 11, SE-41296 Göteborg, Sweden. (johan.mellqvist@chalmers.se)
- J. Jolly, Texas Commission on Air Quality, PO Box 13087, Austin, TX 78711-3087, USA.
- B. Lefer, Department of Geosciences, University of Houston, Houston, 4800 Calhoun Rd., Houston, TX 77204, USA.